electronics

Article

Theory and Experiment of Pulse Wave Rectifier with High Efficiency

Bozhong Xiao [1] and Xuexia Yang [1,2,*]

1 School of Communication and Information Engineering, Shanghai University, Shanghai 200444, China; bozhong@shu.edu.cn
2 Key Laboratory of Specialty Fiber Optics and Optical Access Networks, Shanghai University, Shanghai 200444, China
* Correspondence: yang.xx@shu.edu.cn

Abstract: In this paper, the pulse wave (PW) rectifier of the Schottky diode is theoretically analyzed using the microwave equivalent circuit. It is found that the duty cycle of PW is inversely proportional to the load resistance of the rectifier when the amplitude of the input pulse is the same. Therefore, a stable high-efficiency rectifier can be designed by changing the value of the load resistance when the duty cycles are different. A grounded coplanar waveguide (GCPW) rectifier for the pulse wave is designed to verify this rule. The rectifier is simulated by ADS software and verified by the measurements. When the duty cycle of PW varies from 0.01 to 1 and the input pulse amplitude is stable at the operation frequency of 2.38 GHz, the measured rectifying efficiency can be maintained at the peak efficiency of 76.1% by adjusting the load resistance. However, when the input signal of the rectifier is the continuous wave (CW), the rectifying efficiency is only 3.9% at the same input power amplitude. The proposed rectifier has a simple structure so that it can obtain a high efficiency and has a compact size of $0.22\lambda_0 \times 0.11\lambda_0$. It can be a good candidate for simultaneous wireless information and power transmission (SWIPT) for low-power electronic devices in the Internet of Things (IoT).

Keywords: rectifier; pulse wave; rectifying efficiency; theoretical analysis

check for updates

Citation: Xiao, B.; Yang, X. Theory and Experiment of Pulse Wave Rectifier with High Efficiency. *Electronics* **2022**, *11*, 1274. https://doi.org/10.3390/electronics11081274

Academic Editor: Federico Alimenti

Received: 12 March 2022
Accepted: 15 April 2022
Published: 17 April 2022

1. Introduction

With the rapid development of wireless communication technology, the Internet of Things (IoT), wireless sensor networks (WSNs) and 5G/6G communication are widely studied and applied. Simultaneous wireless information and power transfer (SWIPT) technology is becoming more and more viable and necessary because electronic devices can be wirelessly powered during communication and the battery can be abandoned [1–3]. A rectenna, consisting of a receiving antenna and a rectifier, is the crucial component of the SWIPT system. The rectifier converts the received power efficiently into dc (direct current) energy to power the electronic device. At present, the microwave-direct current (mw-dc) conversion efficiency, called the rectifying efficiency, can reach about 80% [4–6]. Based on the continuous wave (CW), Chang's group proposed the theoretical equations of the input impedance and the rectifying efficiency of the rectifying diode [6]. As is known, only the modulated waves carry the information. Rectifying the modulated waves with a high efficiency is a main feature of SWIPT.

The approaches of designing modulated signal rectifiers can be classified into three types. The first one is measurements. After designing the rectifiers based on the theory of the CW rectifier, the efficiencies of modulated signals were measured [7–11]. The measured peak mw-dc efficiency of the CW in [7] was 78.7%, while that of the QPSK signal was 72.4%. The rectifier in [8] measured a maximum efficiency of 64.6% for CW and a peak efficiency of 61.4% for the BPSK signal. In [9], the CW and AM-PM signal obtained the highest rectifying efficiencies of 52% and 46%, respectively. Apparently, the efficiencies of the modulated waves were lower than that of the CW wave, which is explained by the fact that the peak-to-average power ratios (PAPRs) of the CW and modulated waves were the same. Experimental research has found that the modulated waves with high PAPR would obtain high efficiency when the input power was low [10,11]. Pham et al. measured the maximum efficiencies of 74.7% for pulse wave (PW) and 8.3% for CW when the input power was −15 dBm and the load resistance was 100 kΩ [10]. In [11], the measured results showed that the OFDM, white noise and chaotic signals had a higher efficiency than CW at the input power of −10 dBm.

The second classification is combining simulations with measurements. After simulating the designed rectifiers with ADS software, they were fabricated and measured [12–14]. The mutisine signal obtained a peak efficiency of 72.6% with input power of 16 dBm [12]. The PW rectifier in [13] measured a peak efficiency of 64% under the average input power of 4 dBm, while that in [14] had an efficiency of 59.6% at −2.84 dBm input power.

The third classification is combining theoretical analysis, simulations and measurements. After analyzing the rectifiers theoretically, the conclusions obtained were verified by simulations and measurements. Firstly, the rectifiers were analyzed theoretically. Secondly, the conclusions obtained in the theoretical analysis were verified by simulations and measurements. By providing a theoretical analysis on the load of the rectifier, the authors of [15] concluded that the optimal load of rectifiers for modulated waves would increase with the raise of the wave PAPR. Based on the equivalent circuit model and the derivation in [6], the authors of [16] gave the theoretical formula of rectifying efficiency for power-optimized waveforms when the input PAPR of the rectifier is greater than 1. It was concluded that the efficiency would improve with the input PAPR increasing from 2 to 200 when the input power is low. The theoretical analyses in [15,16] were verified by ADS simulations and measurements.

Apart from the PAPR of the modulated wave, other parameters also influence the peak efficiency of the rectifier. In this paper, the rectifying theory of the PW is analyzed theoretically. It is concluded that maximum efficiency can be obtained when the duty cycle and the load are inversely proportional under the same input PW amplitude. A GCPW (grounded coplanar waveguide) PW rectifier is designed, simulated and measured to validate the rule. The rectifier could be applied in SWIPT systems.

2. Theoretical Analysis of the PW Rectifier

The rectifier of PW is theoretically analyzed taking the voltage doubler rectifier as an example. The equivalent circuit model of the voltage doubler diodes is demonstrated in Figure 1 [17], where R_s is the equivalent series resistance, C_j is the junction capacitance, C_L is the dc filter capacitance and R_L is the load resistance.

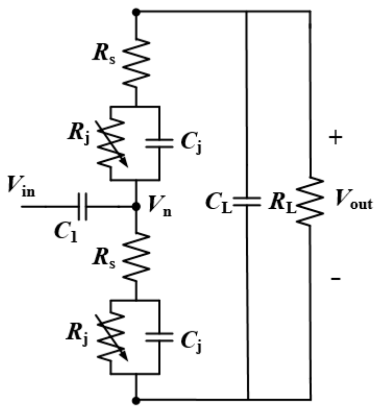

Figure 1. Equivalent circuit model of the voltage doubler diode.

The time-domain waveform of PW with a repetition period of T_a is shown in Figure 2. The CW power is concentrated in a partial duration of ΔT. The ratio of ΔT to T_a is defined as the duty cycle α. The pulse time ΔT contains M consecutive sine periods (M = 3 in Figure 2).

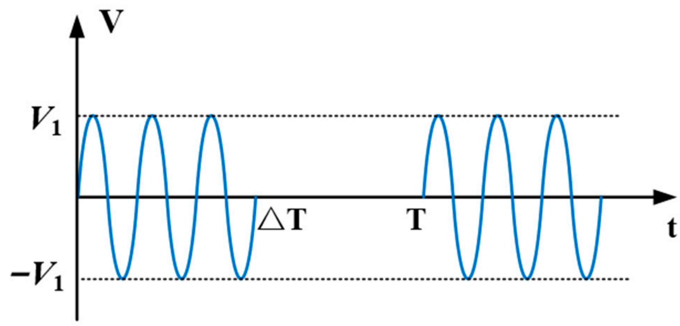

Figure 2. Waveform of PW in the time domain.

The voltage V_d across the diode is given by:

$$V_\mathrm{d} = \begin{cases} -V_{\mathrm{d}0} + V_{\mathrm{d}1}\cos(\omega t - \varphi) & \text{Diodes off and Waveform on} \\ -V_{\mathrm{d}0} & \text{Diodes off and Waveform off} \\ V_\mathrm{T} & \text{Diodes on} \end{cases} \tag{1}$$

in which $V_{\mathrm{d}0}$ is the dc component of V_d across a diode, $V_{\mathrm{d}1}$ is the amplitude of fundamental voltage across the diode, V_T is the forward turn-on voltage of the diode and φ is the phase difference between V_d and V_out, as shown in Figure 3. Assuming that V_0 is the dc component of the voltage across R_L and V_1 is the amplitude of input PW, the voltage V_n of the node between the two diodes is:

$$V_\mathrm{n} = \begin{cases} -\frac{V_0}{2} + V_1\cos(\omega t) & 0 < t < 2\pi M \\ -\frac{V_0}{2} & 2\pi M < t < \frac{2\pi M}{\alpha} \end{cases}. \tag{2}$$

The output voltage V_out is described by:

$$V_\mathrm{out} = \begin{cases} -V_0 + V_1\cos(\omega t) & 0 < \omega t < 2\pi M \\ -V_0 & 2\pi M < \omega t < 2\pi M/\alpha \end{cases} \tag{3}$$

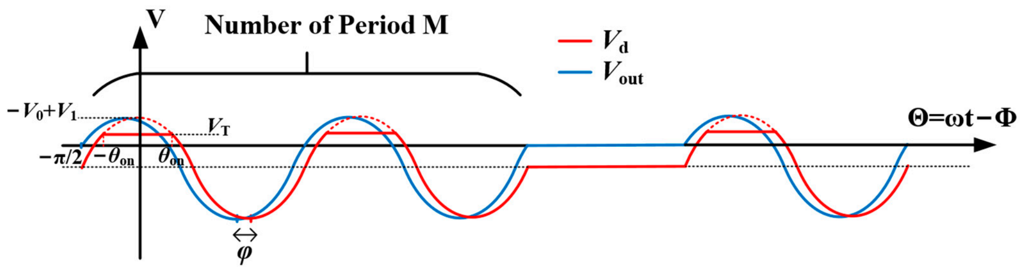

Figure 3. V_d and V_out in the time domain.

$V_\mathrm{d,dc}$ is the average value of V_d in a complete period. It can be calculated by:

$$\begin{gathered} V_\mathrm{d,dc} = \frac{1}{T}\int_0^T V_\mathrm{d} d\theta = \frac{1}{2\pi M/\alpha}\int_{-\frac{\pi}{2}}^{\frac{2\pi M}{\alpha}-\frac{\pi}{2}} V_\mathrm{d} d\theta \\ = \frac{\alpha}{2\pi}\left[-2V_{\mathrm{d}1}\sin\theta_\mathrm{on} + 2V_{\mathrm{d}0}\theta_\mathrm{on} - 2V_\mathrm{T}\theta_\mathrm{on} - \frac{2\pi V_{\mathrm{d}0}}{\alpha}\right] \end{gathered} \tag{4}$$

in which $\theta = \omega t - \varphi$ and θ_on is the phase angle that the diode is turned on. It is obvious that the value of M is eliminated in (5), which indicates that M is unrelated to $V_\mathrm{d,dc}$.

According to the Kirchhoff law, the output dc voltage and the voltage across the diode have the relationship:

$$\frac{V_0}{2} = \frac{V_\mathrm{d,dc}}{1 + 2 \times R_\mathrm{s}/R_\mathrm{L}}. \tag{5}$$

The input voltage and current should be described as the root mean square (RMS) value. The RMS voltage of fundamental is calculated in:

$$V_{\mathrm{RMS}} = \sqrt{\frac{1}{T}\int V^2(\theta)d\theta} = \sqrt{\frac{\alpha}{2\pi}\int_{\frac{-\pi}{2}}^{\frac{3\pi}{2}} (V_1\cos(\theta+\varphi))^2 d\theta} = V_1\sqrt{\frac{\alpha}{2}} \tag{6}$$

The current across each diode is complex, so it is illustrated as:

$$I = I_{\mathrm{R}}\cos(\theta) + I_{\mathrm{i}}\sin(\theta) \tag{7}$$

in which only the real part $I_{\mathrm{R}}\cos(\theta)$ is taken into account because the imaginary part does not consume electric energy. The real current is:

$$\begin{aligned} I_{\mathrm{R}} = \tfrac{1}{\pi R_{\mathrm{s}}}[\textstyle\int_{\frac{-\pi}{2}}^{-\theta_{\mathrm{on}}} (V-V_{\mathrm{d}})\cos(\theta+\varphi)d\theta + \int_{-\theta_{\mathrm{on}}}^{\theta_{\mathrm{on}}} (V-V_T)\cos(\theta+\varphi)d\theta \\ +\textstyle\int_{\theta_{\mathrm{on}}}^{\frac{3\pi}{2}} (V-V_{\mathrm{d}})\cos(\theta+\varphi)d\theta] = I_{\mathrm{R}}(\theta_{\mathrm{on}},\varphi) \end{aligned} \tag{8}$$

where I_{R} $(\theta_{\mathrm{on}}, \varphi)$ is a function of θ_{on} and φ. Therefore, the RMS current across each diode is:

$$I_{\mathrm{RMS}} = \sqrt{\frac{\alpha}{2\pi M}\int_{-\frac{\pi}{2}}^{\frac{3\pi}{2}} M\times(I_{\mathrm{R}}\cos\theta)^2 d\theta} = I_{\mathrm{R}}(\theta_{\mathrm{on}},\varphi)\sqrt{\frac{\alpha}{2}}. \tag{9}$$

The total input power can be obtained as:

$$P_{\mathrm{in}} = V_{\mathrm{RMS}}(2I_{\mathrm{RMS}}). \tag{10}$$

Hence, the rectifying efficiency η is described as:

$$\eta = \frac{P_{\mathrm{out}}}{P_{\mathrm{in}}} = \frac{V_0^2/R_{\mathrm{L}}}{V_{\mathrm{RMS}}(2I_{\mathrm{RMS}})} = \frac{V_0^2}{V_1 I_{\mathrm{R}}(\theta_{\mathrm{on}},\varphi)\alpha R_{\mathrm{L}}} = \eta(\alpha R_{\mathrm{L}}). \tag{11}$$

It can be found from Equation (11) that the rectifying efficiency of a PW rectifier is related to the production of the duty cycle α and the load resistance R_{L}. When the peak input voltage V_1 remains a constant value and the product of α and R_{L} does not change, the maximum efficiency of the rectifier remains unchanged. In other words, under different duty cycles, the PW rectifier can maintain high rectifying efficiency by changing the load. CW can be regarded as a special PW with the duty cycle α being 1. Once the optimal load of the CW rectifier R_{LCW} and that of the PW rectifier R_{LPW} have the relationship $R_{\mathrm{LCW}} = \alpha \times R_{\mathrm{LPW}}$, the peak rectifying efficiencies of the two types of waveforms are the same when the amplitude remains the same.

The rectifying efficiency of PW rectifier is calculated using the following formula:

$$\eta = \frac{V_0^2/R_{\mathrm{L}}}{P_{\mathrm{in}}}. \tag{12}$$

Considering a duty cycle of PW, the input pulse power P_{pw} and the average input power P_{in} have the following relationship:

$$P_{\mathrm{in}} = P_{\mathrm{pw}} + 10\log(\alpha)\ (\mathrm{dBm}). \tag{13}$$

In the view of power, P_{in} should be applied while calculating PW's rectifying efficiency. It can be concluded that PW can obtain a higher efficiency at low average input power because the PW concentrates the power of CW in a partial time so that it can obtain a higher amplitude under the same relatively low value of P_{in}.

3. PW Rectifier Design and Measurement

In order to verify the conclusions drawn from the theoretical analysis of PW rectification in the previous section, a PW rectifier is designed. The schematic of a voltage doubling rectifier is shown in Figure 4. The rectifier consists of an impedance matching network, two rectifying diodes, a dc filter and a load resistance.

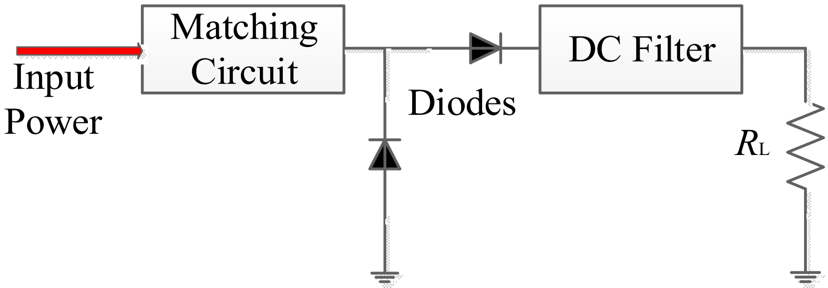

Figure 4. Schematic of the voltage doubling rectifier.

The structure of the designed rectifier is presented in Figure 5. The GCPW transmission line is employed in the proposed rectifier to provide a dc path to diodes without vias, which have parasitic effects in rectifiers using microstrip lines. The Schottky diode HSMS-2862 is selected as the rectifying diode. HSMS-2862 consists of two diodes of HSMS-2860, which has a low junction capacitance of C_{j0} = 0.18 pF, a low forward bias voltage of V_T = 0.35 V and a reverse breakdown voltage of V_{br} = 4 V [18]. The series capacitor C_1 with a value of 47 pF acts as a dc block to prevent the dc signal from flowing back to the input source. To suppress the high-order harmonics and smooth the output dc voltage, the dc filter is designed by using capacitors C_2 and C_3 with a value of 470 pF, which are connected in parallel across the GCPW transmission line. The substrate is F4B with the relative dielectric constant ε_r of 2.65, the loss tangent tanδ of 0.001 and thickness h of 0.8 mm. The rectifier is simulated using ADS software. The parameters of the rectifier are w_1 = 2.1 mm, w_2 = 0.7 mm, w_3 = 4 mm, g_1 = 1 mm and g_2 = 1.7 mm. The proposed rectifier operates at 2.4 GHz and has a compact size of 0.22 λ_0 × 0.11 λ_0 (28 × 14 mm^2).

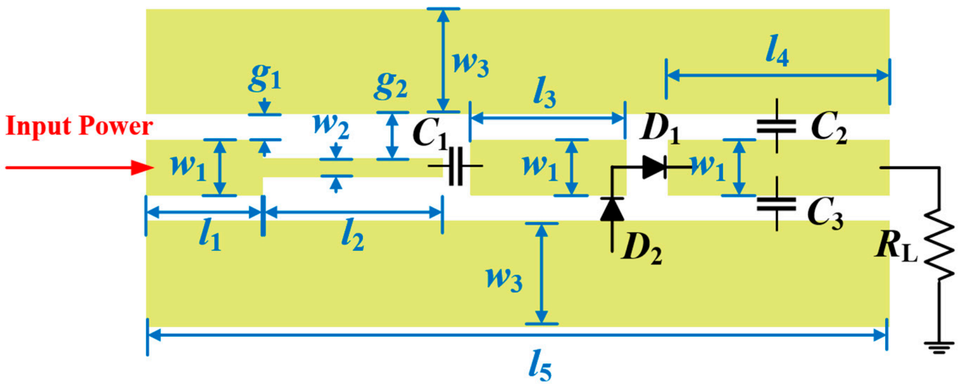

Figure 5. Structure of the proposed rectifier.

The schematic and the actual measurement system are shown in Figure 6. CW and PW are both generated by the signal source AV1431. The output voltage across the load was measured with a voltage meter.

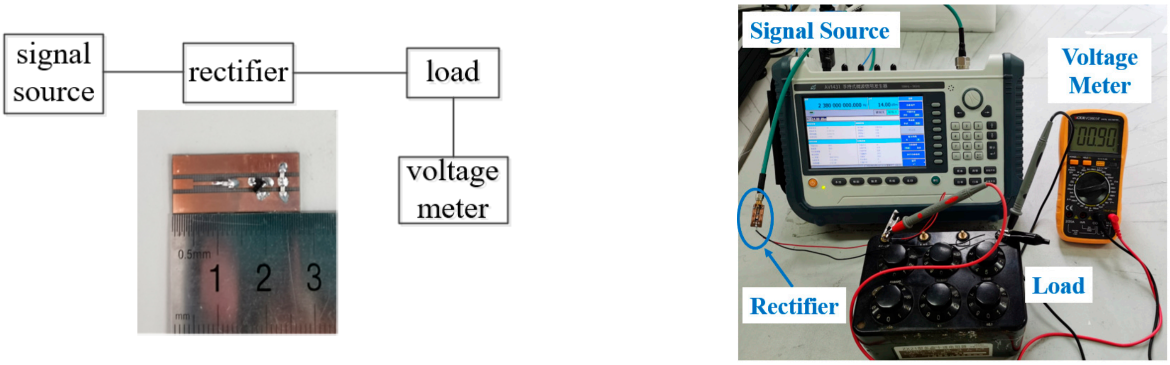

(**a**) (**b**)

Figure 6. Measurement system of the rectifier: (**a**) schematic (**b**) actual.

3.1. Measurements under the Same Voltage Amplitude

When the peak input voltage of the rectifier is the same, the rectifying efficiency versus load under different duty cycles is illustrated in Figure 7. Good agreement is achieved between simulated and measured results. The simulated operating frequency of the rectifier is 2.4 GHz as the input pulse power P_{pw} is 17 dBm. The average input power P_{in} can be calculated according to (13). The highest simulated rectifying efficiency remains above 77%, at the duty cycles of 0.01, 0.1, 0.5 and 1 and the corresponding loads of 50 kΩ, 5 kΩ, 1 kΩ and 0.5 kΩ. With the increase of duty cycle, the corresponding optimal load value decreases and the inverse relationship between the duty cycle and the load is satisfied. As the measured operating frequency is 2.38 GHz and the optimal input power P_{pw} is 20 dBm, the highest rectifying efficiency is generally maintained at 76%. The corresponding loads are 50 kΩ, 5 kΩ, 1 kΩ and 0.5 kΩ. Compared with the simulation results, the measured maximum rectifying efficiency is slightly decreased, but the trend of the curve remains the same. The diodes, capacitors and SMA connector are all soldered manually by ourselves, which leads to parasitic effects such as parasitic capacitors and inductances in the experimental measurements. Parasitic effects may cause the frequency offset. Therefore, the simulated and measured frequencies are 2.4 GHz and 2.38 GHz, respectively.

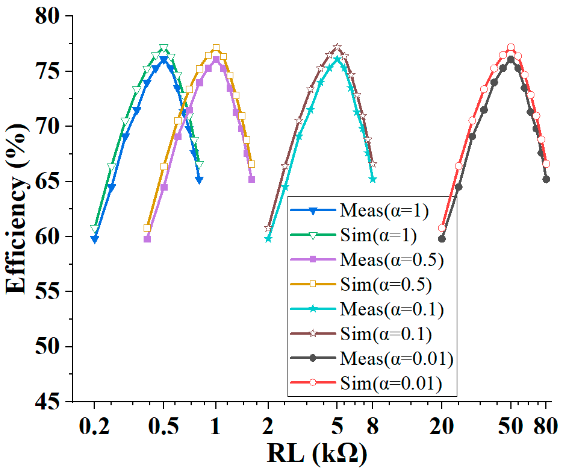

Figure 7. Simulation and measurement of rectifying efficiency at the same input voltage.

Figure 8 shows the relationship between the duty cycle α and the load R_L through calculations (shown in Appendix A), simulations and measurements when the PW rectifier reaches the maximum rectifying efficiency and the input voltage is stable. It is observed that when the PW rectifier obtains the highest rectifying efficiency under the same input voltage amplitude, the duty cycle α is proportional to the load reciprocal $1/R_L$ so that the product of α and R_L is a fixed value, which verifies the theoretical analysis.

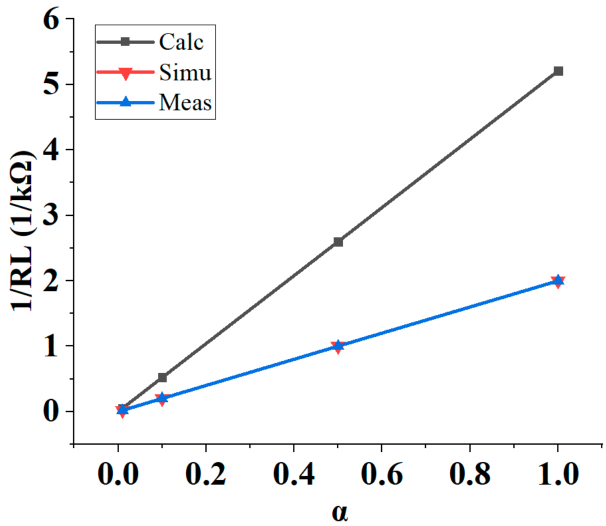

Figure 8. $1/R_L$ versus α at the same input voltage under the peak rectifying efficiency.

3.2. Measurements under the Same Average Input Power

Under different duty cycles, the efficiency of the rectifier varying with the load under the same average input power P_{in} is shown in Figure 9. The simulated operating frequency of the rectifier is 2.4 GHz and the measured frequency is 2.38 GHz. The simulated and measured average input power are –3 dBm and 0 dBm, respectively. The load range is 20–80 kΩ. As the duty cycle increases, the highest rectification efficiency gradually decreases. Compared with the simulation results, the actual measurement has the same change trend and the efficiency is slightly reduced. When α and R_L are 0.01 and 50 kΩ, respectively, the highest rectification efficiency is 76.1%.

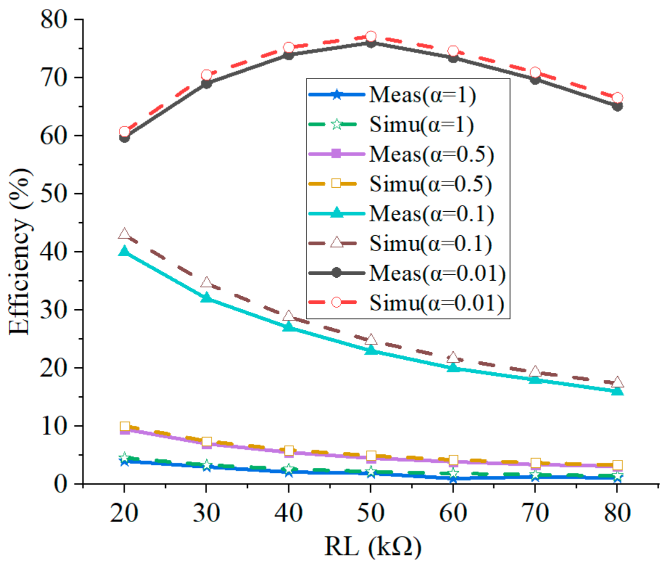

Figure 9. Simulation and measurement of rectifying efficiency at the same average input power.

3.3. Formatting of Mathematical Components

Under different duty cycles, the rectifying efficiency versus the average input power is shown in Figure 10. The measured operating frequency is 2.38 GHz, the load is 50 kΩ and the values of duty cycle α are 0.01, 0.1 and 1. When the duty cycle is 0.01, the measured highest rectifying efficiency is 76.1%, which is much greater than the highest rectification efficiencies of 3.9% and 28.4% when α is 1 and 0.1, respectively.

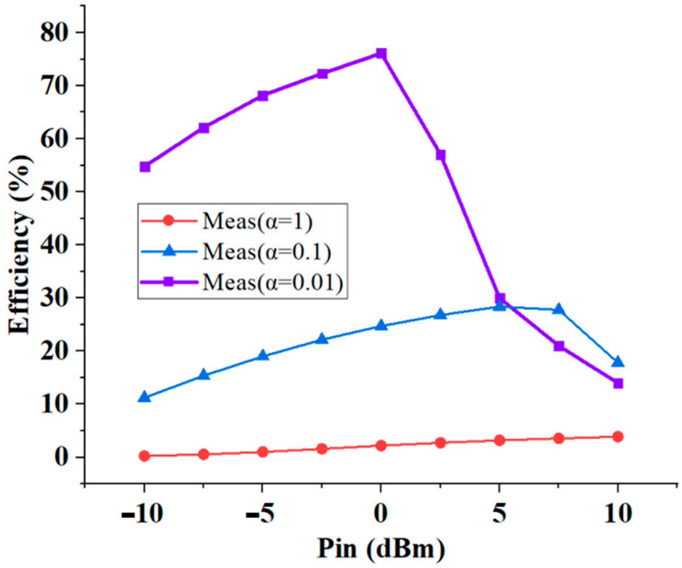

Figure 10. Measurement of rectifying efficiency at the same load resistance.

4. Discussions

According to measurements under the same voltage amplitude, the conclusion of theoretical analysis is verified. When the peak input voltage is maintained, the peak rectifying efficiency of the PW remains unchanged and the product of α and R_L is a fixed value. CW can be regarded as a special PW with the duty cycle α being 1. Therefore, a CW rectifier can be changed into a PW rectifier by changing the duty cycle and load.

The measured optimal input power and load corresponding to $\alpha = 1$ are $P_{in} = 20$ dBm and $R_L = 0.5$ kΩ, respectively, while those corresponding to $\alpha = 0.01$ are $P_{in} = 20 + 10\log 0.01 = 0$ dBm and $R_L = 50$ kΩ when the peak efficiencies are obtained. Therefore, the PW rectifier has a rectifying efficiency higher than 76% in the input power range of 0–20 dBm and the load range of 0.5–50 kΩ when α varies from 0.01 to 1. It is known that when the input voltages of PW and CW are the same, the duty cycle and load can be adjusted to obtain high rectifying efficiency in a wide input power range and a wide load range.

From measurements under the same input power and the same load, it can be concluded that due to the concentrated energy of PW, the rectification efficiency of PW is greater than that of CW ($\alpha = 1$) under the conditions of low input power and high load resistance.

The performances of PW rectifiers in the literature are summarized in Table 1. It can be observed that this work has the following advantages. First, the PW rectifier is analyzed theoretically. It is concluded that the duty cycle of PW is inversely proportional to the load resistance of the rectifier when the amplitude of the input pulse is the same. The conclusion is validated by simulations and measurements. Second, the proposed rectifier has a simple structure so that the efficiency exceeds those in the literature and the size is compact.

Table 1. Comparison of the proposed PW rectifier with others in the literature.

References	Diode	Load (Ω)	Size (λ_0)	Material	Voltage [1] (V)	Efficiency (%)	Theoretical Analysis
[10]	SMS-7630	100k	N/A	FR4	N/A	74.7	N/A
[13]	SMS-7621	N/A	N/A	FR4	N/A	64	N/A
[14]	Cockcroft–Walton type	20k	N/A	Rogers RO4003C	N/A	59.6	N/A
This Work	HSMS-2862	50k	0.22×0.11	F4B	6.17	76.1	Studied and validated

[1] The voltage corresponds to the peak efficiency instead of the highest voltage.

5. Conclusions

This paper studies PW rectification theoretically and designs a GCPW rectifier that obtains high-efficiency rectification. Based on the theory of the rectifier, the efficiency of PW rectification is analyzed. When the amplitude of the input voltage is the same, the inverse relationship between the duty cycle and the load is obtained. Therefore, high-efficiency rectification can be obtained under different duty cycles by changing the load. The rectifier adopts a voltage-doubling topology and a transmission line of ground coplanar waveguide. When the measured operating frequency is 2.38 GHz, the average input power is 0 dBm, the load is 50 kΩ and the duty cycle is 0.01, the highest rectifying efficiency reaches 76.1%. CW (α = 1), which has the same amplitude, has an equal highest rectifying efficiency at 500 Ω. In addition, PW can obtain a higher rectifying efficiency than CW under low input power and high load conditions. In the future, research on the PW rectifier can expand the application range of microwave power transmission and can be combined with information transmission to realize SWIPT.

Author Contributions: Conceptualization, B.X.; experiment design, B.X.; experiment performance, B.X.; data analysis, B.X. and X.Y.; writing—original draft preparation, B.X. and X.Y. All authors have read and agreed to the published version of the manuscript.

Funding: This research was funded by the National Natural Science Foundation of China, grant number 62171270.

Institutional Review Board Statement: Not applicable.

Informed Consent Statement: Not applicable.

Data Availability Statement: The data presented in this study are openly available.

Conflicts of Interest: The authors declare no conflict of interest.

Appendix A

The theoretical analysis in Section 2 can be verified as follows. The phase angle θ_{on} is described by:

$$\cos(\theta_{\mathrm{on}}) = \frac{V_{\mathrm{T}} + V_{\mathrm{d0}}}{V_{\mathrm{d1}}}. \tag{A1}$$

Assume that the junction resistance of the diode is very large when the diode is off. Therefore, the voltage across the series resistance R_{s} is shown by:

$$R_{\mathrm{s}} \frac{d(C_{\mathrm{j}} V_{\mathrm{d}})}{dt} = V_{\mathrm{n}} - V_{\mathrm{d}}. \tag{A2}$$

The junction capacitance C_{j} is calculated by taking a Fourier series where:

$$C_{\mathrm{j}} \approx C_0 + C_1 \cos(\omega t - \varphi) + C_2 \cos(2\omega t - 2\varphi) + \ldots \tag{A3}$$

in which the term higher than the second harmonic can be neglected. Substituting (A3) into (A2), it can be seen that:

$$\omega R_{\mathrm{s}}(C_1 V_{\mathrm{d0}} - C_0 V_{\mathrm{d1}}) \sin(\omega t - \varphi) = V_{\mathrm{d0}} - \frac{V_0}{2} + (V_1 \cos(\varphi) - V_{\mathrm{d1}}) \cos(\omega t - \varphi) - V_1 \sin\varphi \sin(\omega t - \varphi). \tag{A4}$$

Since (A4) should hold during the off period of the diode, each term in (A4) is separately zero:

$$V_{\mathrm{d0}} = \frac{V_0}{2} \tag{A5}$$

$$V_{\mathrm{d1}} = V_1 \cos(\varphi). \tag{A6}$$

Substituting (5) and (A4) into (A6), φ is described as:

$$\varphi = \arctan\left[\omega R_{\mathrm{s}}\left(C_0 - \frac{C_1 \cos(\theta_{\mathrm{on}})}{1 + V_{\mathrm{T}}/(V_0/2)} + C_2\right)\right] \approx \arctan(\omega R_{\mathrm{s}} C_{\mathrm{eff}}) \tag{A7}$$

in which C_{eff} is the effective capacitance and can be seen as $C_{\mathrm{eff}} \approx C_{\mathrm{j}}$ [16].

The relationship between θ_{on}, R_s, R_L and α is obtained by substituting (5), (A1), (A5) and (A6) into (4), so it is shown as:

$$\frac{\pi R_s/(\alpha R_L)}{1+V_T/(V_0/2)} = \tan(\theta_{on}) - \theta_{on}. \tag{A8}$$

V_1 is calculated according to:

$$P_{PW} = \frac{V_{1eff}^2}{Z_{in}} \tag{A9}$$

where V_{1eff} is the effective value of input voltage and the relationship between V_{1eff} and V_1 is $V_1 = \sqrt{2}V_{1eff}$.

When the input impedance Z_{in} is matched with the internal resistance Z_s of the signal source, its value is:

$$Z_{in} = Z_s^* = 50\ \Omega. \tag{A10}$$

P_{pw} = 20 dBm is substituted into (A9) and (A10) to obtain V_1 = 3.16 V.

Taking $C_{eff} \approx C_{j0}$, substituting frequency f = 2.4 GHz, diode's junction resistance R_s = 6 Ω and the zero-bias capacitance C_{j0} = 0.18 pF into Formula (A7), the phase difference φ = 0.0163 can be obtained.

In order to obtain the highest rectifying efficiency, the output voltage is V_0 = V_{br} = 4 V [16]. V_T = 0.35 V, (A5) and (A6) are substituted into (A1) to obtain the conduction angle θ_{on} = 0.7329. Different duty cycles α can be substituted into (A8) to obtain the corresponding load resistance R_L for different values of α so that the result of the calculation in Figure 8 is obtained.

Finally, substituting all the known conditions above and using (13), the theoretical maximum rectifying efficiency of PW under different duty cycles is obtained. The calculated peak rectifying efficiency is 83.4%.

References

1. Jin, Y.; Kwak, K.S.; Yoo, S.-J. A Novel Energy Supply Strategy for Stable Sensor Data Delivery in Wireless Sensor Networks. *IEEE Syst. J.* **2020**, *14*, 3418–3429. [CrossRef]
2. Gustavsson, U.; Frenger, P.; Fager, C.; Eriksson, T.; Zirath, H.; Dielacher, F.; Studer, C.; Pärssinen, A.; Correia, R.; Matos, J.N.; et al. Implementation Challenges and Opportunities in Beyond-5G and 6G Communication. *IEEE J. Microw.* **2021**, *1*, 86–100. [CrossRef]
3. Ponnimbaduge Perera, T.D.; Jayakody, D.N.K.; Sharma, S.K.; Chatzinotas, S.; Li, J. Simultaneous Wireless Information and Power Transfer (SWIPT): Recent Advances and Future Challenges. *IEEE Commun. Surv. Tutor.* **2018**, *20*, 264–302. [CrossRef]
4. Rodenbeck, C.T.; Jaffe, P.I.; Strassner, B.H., II; Hausgen, P.E.; McSpadden, J.O.; Kazemi, H.; Shinohara, N.; Tierney, B.B.; DePuma, C.B.; Self, A.P. Microwave and Millimeter Wave Power Beaming. *IEEE J. Microw.* **2021**, *1*, 229–259. [CrossRef]
5. Chen, Z.N.; Liu, D.; Nakano, H.; Qing, X.; Zwick, T. Antennas in Microwave Wireless Power Transmission. In *Handbook of Antenna Technologies*; Springer Publishing Company: Berlin/Heidelberg, Germany, 2016; pp. 3033–3076.
6. Yoo, T.; Chang, K. Theoretical and experimental development of 10 and 35 GHz rectennas. *IEEE Trans. Microw. Theory Tech.* **1992**, *40*, 1259–1266. [CrossRef]
7. Zhu, G.; Du, J.; Yang, X.; Zhou, Y.; Gao, S. Dual-Polarized Communication Rectenna Array for Simultaneous Wireless Information and Power Transmission. *IEEE Access* **2019**, *7*, 141978–141986. [CrossRef]
8. Jiang, Z.; Wang, Z.; Leach, M.; Lim, E.G.; Zhang, H.; Pei, R.; Huang, Y. Symbol-Splitting-Based Simultaneous Wireless Information and Power Transfer System for WPAN Applications. *IEEE Microw. Wirel. Compon. Lett.* **2020**, *30*, 713–716. [CrossRef]
9. Rajabi, M.; Pan, N.; Claessens, S.; Pollin, S.; Schreurs, D. Modulation Techniques for Simultaneous Wireless Information and Power Transfer with an Integrated Rectifier–Receiver. *IEEE Trans. Microw. Theory Tech.* **2018**, *66*, 2373–2385. [CrossRef]
10. Pham, V.-D.; Takhedmit, H.; Cirio, L. Waveform Optimization Using RF Pulse Signal on Voltage-Doubler Broadband Rectenna. *IEEE J. Rad. Freq. Ident.* **2021**, *5*, 139–147. [CrossRef]
11. Collado, A.; Georgiadis, A. Optimal Waveforms for Efficient Wireless Power Transmission. *IEEE Microw. Wirel. Compon. Lett.* **2014**, *24*, 354–356. [CrossRef]
12. Liu, Z.; Zhong, Z.; Guo, Y. In Vivo High-Efficiency Wireless Power Transfer with Multisine Excitation. *IEEE Trans. Microw. Theory Tech.* **2017**, *65*, 3530–3540. [CrossRef]
13. Ibrahim, R.; Voyer, D.; Zoghbi, M.E.; Huillery, J.; Bréard, A.; Vollaire, C.; Allard, B.; Zaatar, Y. Novel Design for a Rectenna to Collect Pulse Waves at 2.4 GHz. *IEEE Trans. Microw. Theory Tech.* **2018**, *66*, 357–365. [CrossRef]
14. Yang, C.; Yang, Y.; Lo, C. Subnanosecond Pulse Generators for Impulsive Wireless Power Transmission and Reception. *IEEE Trans. Circuits Syst. Express Briefs* **2011**, *58*, 817–821. [CrossRef]

15. Bolos, F.; Blanco, J.; Collado, A.; Georgiadis, A. RF Energy Harvesting from Multi-Tone and Digitally Modulated Signals. *IEEE Trans. Microw. Theory Tech.* **2016**, *64*, 1918–1927. [CrossRef]
16. Valenta, C.R.; Morys, M.M.; Durgin, G.D. Theoretical Energy-Conversion Efficiency for Energy-Harvesting Circuits Under Power-Optimized Waveform Excitation. *IEEE Trans. Microw. Theory Tech.* **2015**, *63*, 1758–1767. [CrossRef]
17. Valenta, C.R.; Peterson, C.W. Theoretical energy-conversion efficiency for multi-stage RF energy harvesters. In Proceedings of the IEEE International Conference on RFID (RFID), Orlando, FL, USA, 3–5 May 2016.
18. HSMS-286x Surface Mount RF Schottky Barrier Diodes. Available online: https://html.alldatasheetcn.com/html-pdf/729560/AVAGO/HSMS-2862/310/2/HSMS-2862.html (accessed on 12 March 2022).